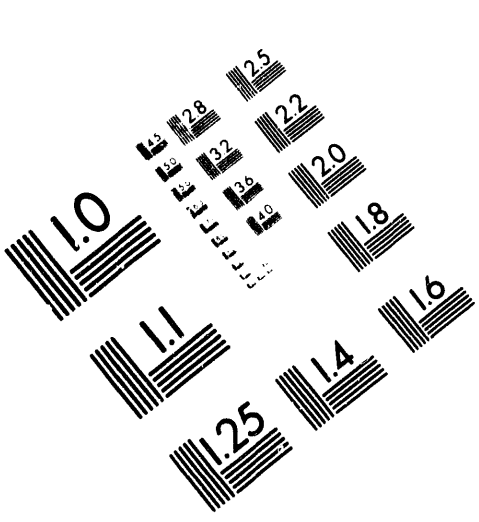

Association for Information and Image Management
1100 Wayne Avenue, Suite 1100
Silver Spring, Maryland 20910
301/587-8202

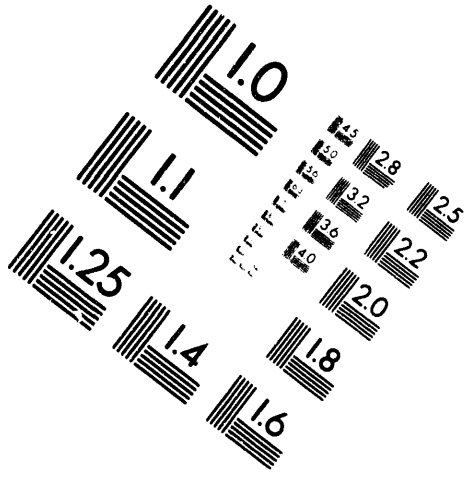

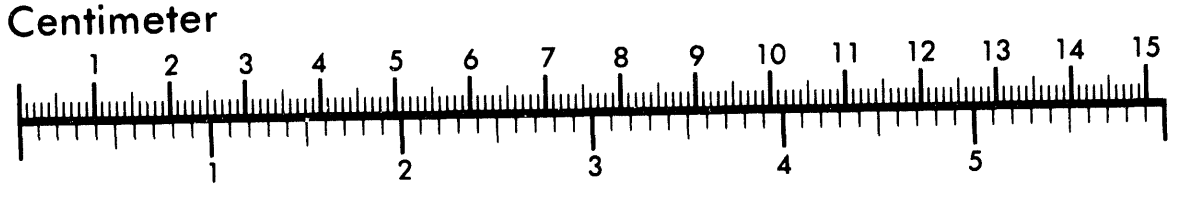

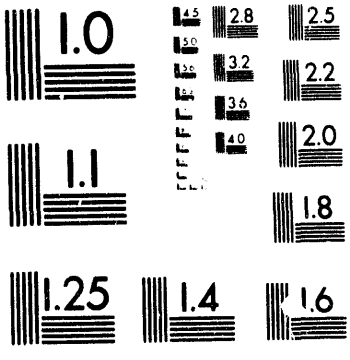

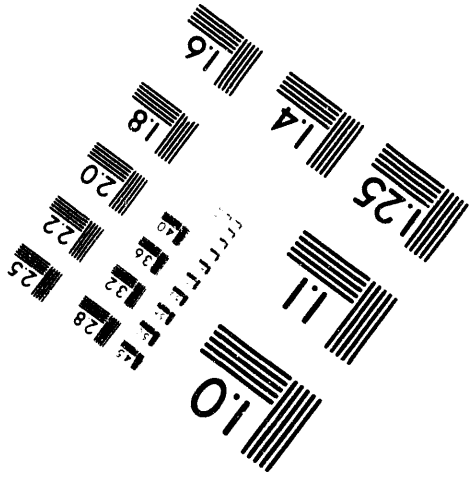

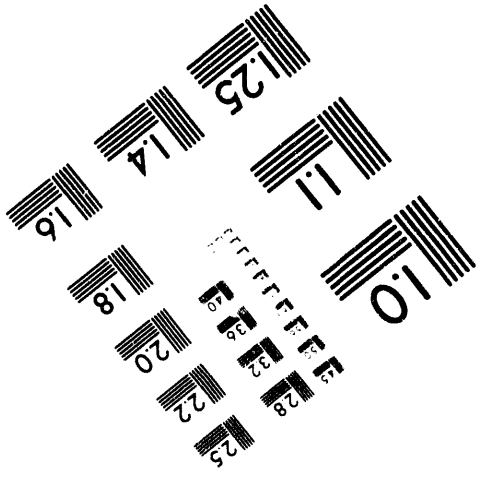

MANUFACTURED TO AIIM STANDARDS
BY APPLIED IMAGE, INC.

1 of 1

LA-UR- 94-2761

Conf-9405216--1

Title: **Neutrino Oscillation Studies at LAMPF**

Author(s): **W. C. Louis**

Submitted to: ***Proc. of Neutrino 94, XVI International Conference on Neutrino Physics and Astrophysics***
Eilat, Red Sea, Israel, May 29–June 3, 1994

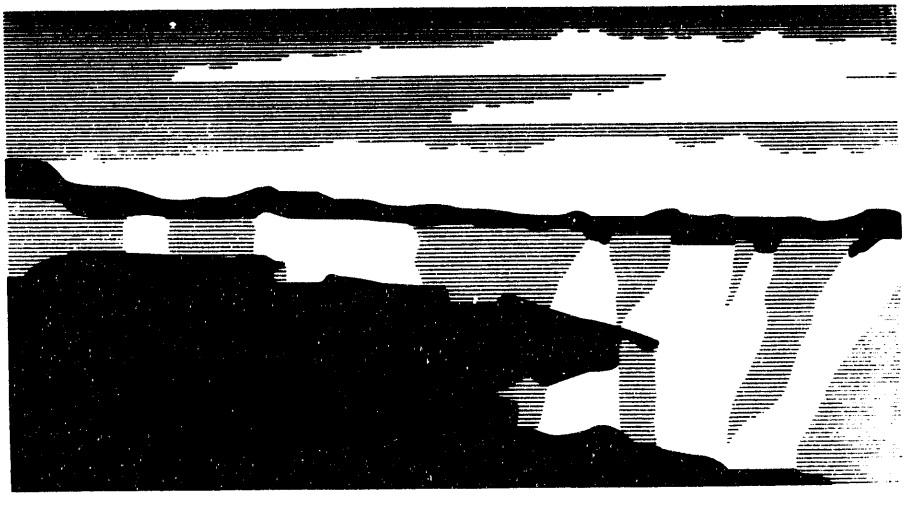

Los Alamos
NATIONAL LABORATORY

Form No. 836 R5
ST 2629 10/91

Neutrino oscillation studies at LAMPF

W. C. Louis, representing the LSND Collaboration [1]
Los Alamos National Laboratory, Physics Division
Los Alamos, NM 87545, U.S.A.

A search for $\bar{\nu}_\mu \to \bar{\nu}_e$ oscillations has been made by the Liquid Scintillator Neutrino Detector experiment at LAMPF after an initial month and a half run. The experiment observes eight events consistent with the reaction $\bar{\nu}_e p \to e^+ n$ followed by $np \to d\gamma$ (2.2 MeV). The total estimated background is 0.9 ± 0.2 events.

1. INTRODUCTION

Neutrino production from π and μ decay at rest from the LAMPF beam stop is expected to arise almost entirely from $\pi^+ \to \mu^+ \nu_\mu$ and $\mu^+ \to e^+ \bar{\nu}_\mu \nu_e$ decays. Neutrinos from π^- and μ^- decays are suppressed due to the smaller π^- yield and to the high capture probability in the Fe and Cu of the beam stop. Therefore, the observation of significant $\bar{\nu}_e$ production would be evidence for new physics such as $\bar{\nu}_\mu \to \bar{\nu}_e$ oscillations, which would imply that neutrinos have mass (and cosmological significance) and that there is mixing among the lepton families.

2. LSND EXPERIMENT

The Liquid Scintillator Neutrino Detector (LSND) experiment makes use of the LAMPF neutrino beam and consists of a cylindrical tank approximately 8.5-m-long by 5.5-m in diameter. On the inside surface of the tank are mounted 1220 8-inch Hamamatsu phototubes, 25% of the surface area is covered by photocathode, and the tank is filled with 51,000 gallons (180 tons) of liquid scintillator consisting of mineral oil and 0.031 g/ℓ of b-PBD. The low scintillator concentration allows the detection of both Čerenkov light and scintillation light and yields a relatively long attenuation length of more than 20 m for wavelengths greater than 400 nm. Surrounding the detector tank is a liquid-scintillator veto shield [2] with 292 5-inch phototubes that tag cosmic muons passing through the detector. A 45-MeV electron created in the detector produces about 370 photoelectrons in the Čerenkov cone and 1115 photoelectrons isotropically [3] and is reconstructed with a position resolution of ~25 cm, an angular resolution of ~15°, and an energy resolution of ~6%. In addition, particle identification for particles above and below Čerenkov threshold is obtained through the fit to the Čerenkov cone and from the time distribution of the light, which is relatively later for particles below Čerenkov threshold. Figure 1(a) shows the energy distribution for a sample of Michel electrons from cosmic muon decays in the tank, from which is obtained the electron energy resolution and calibration. The solid curve is a fit with the Michel electron spectrum convoluted by a Gaussian resolution of $42\%/\sqrt{(E\ (\mathrm{MeV}))}$ and an end-point energy of 52.8 MeV corresponding to about 1740 photoelectrons (~33 photoelectrons per MeV).

The detector is located at a mean distance of 29 m from the A6 LAMPF beam stop and at an average angle of 12° relative to the incident proton direction. The beam stop

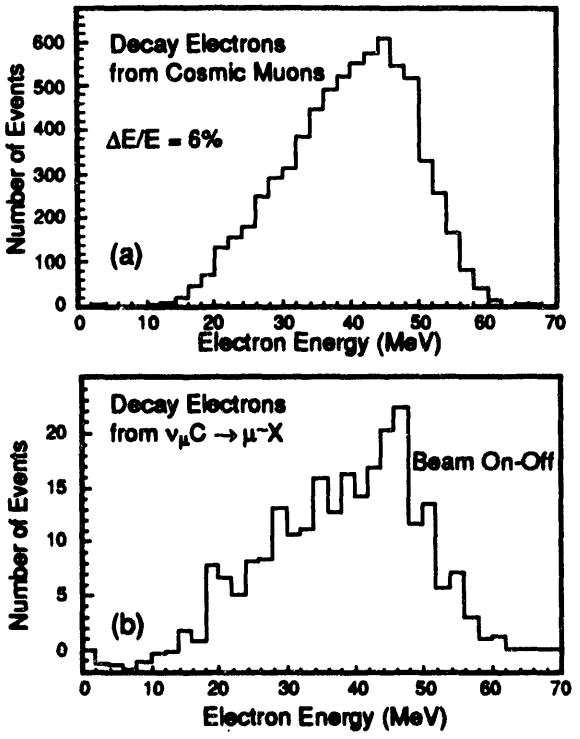

Figure 1. (a) The energy distribution for a sample of Michel electrons from cosmic muon decays in the tank, from which is obtained the energy resolution and calibration. The solid curve is a fit with the decay electron spectrum convoluted by a Gaussian resolution of $42\%/\sqrt{(E\ (\mathrm{MeV}))}$ and an endpoint energy at 52.8 MeV corresponding to 1740 photoelectrons. (b) The energy distribution for a sample of over 200 electrons from muon decay where the muons are produced by the reaction $\nu_\mu C \rightarrow \mu^- X$.

consists of a 20-cm water target positioned 1 m upstream of a water-cooled Cu beam dump. Approximately 20% of the protons in the LAMPF beam interact in the upstream targets A1 and A2, located 120 m and 100 m from the detector, allowing 80% of the LAMPF beam to interact at A6. The neutrinos arise from pion and muon decay and can be separated into those from decay in flight and those from decay at rest. The π^+ and μ^+ decay-at-rest neutrino energy spectra extend up to 52.8 MeV, while the pion decay-in-flight spectrum has an average energy of 100 MeV with a high energy distribution extending beyond 250 MeV. As π^- produced in the beam stop are strongly absorbed, the decay-at-rest neutrino flux is almost entirely due to ν_μ from π^+ decay and $\bar{\nu}_\mu$ and ν_e from μ^+ decay. The neutrino flux is calculated from measured pion cross sections [4], and the uncertainty in the decay-at-rest and decay-in-flight neutrino fluxes are estimated to be 7% and 12%, respectively. There is no uncertainty in the decay-at-rest neutrino energy shape, while the uncertainty in the decay-in-flight energy shape is included in the flux uncertainty.

The average proton intensity at the A6 beam-stop was ~700 μA during a 1.5-month run in the autumn of 1993, and the average beam duty factor was 7%. The data sample corresponds to an exposure of 1800 Coulombs of protons on the A6 beam stop, resulting in a total decay-at-rest neutrino flux of 9×10^{13} ν/cm^2 at the center of the tank. The primary trigger threshold was 100 hit phototubes. After a primary trigger with >300 hit phototubes, the threshold was lowered to 21 hit phototubes for a period of 1 ms in order to trigger on 2.2-MeV γ from neutron capture on free protons. In addition, all past activities within 50 μs of a primary event with >17 hit detector phototubes or >5 hit veto shield phototubes were recorded. Furthermore, no primary triggers were allowed for a period of 15 μs following veto shield events with >5 hit veto phototubes in order to reject the decay electrons following stopped cosmic muons. The total trigger deadtime, due to data that get overwritten in memory before they can be read out, is estimated to be $2 \pm 1\%$.

3. RESULTS

Figure 1(b) shows the energy distribution for a sample of 216 Michel electrons from muon decay where the muons are produced by the reaction $\nu_\mu C \rightarrow \mu^- X$. This sample enables us to make the first accurate measurement of the $\nu_\mu C \rightarrow \mu^- X$ cross section near threshold, and the cross section obtained is less than half of the Fermi Gas Model prediction [5]. Figure 2(a) shows the electron energy distributions resulting from $\nu_e\ ^{12}C \rightarrow e^-\ ^{12}N$ scattering, $\nu_e\ ^{13}C \rightarrow e^-\ ^{13}N$ scattering, and $\nu e \rightarrow \nu e$ elastic scattering. The data agree with the expected number of events shown as dots in the figure. Figure 2(b) shows the $\cos\theta$ distribution for these same events, where θ is the angle between the electron direction and the incoming neutrino direction. The excess of events near $\cos\theta = 1$ is due to $\nu e \rightarrow \nu e$ elastic scattering.

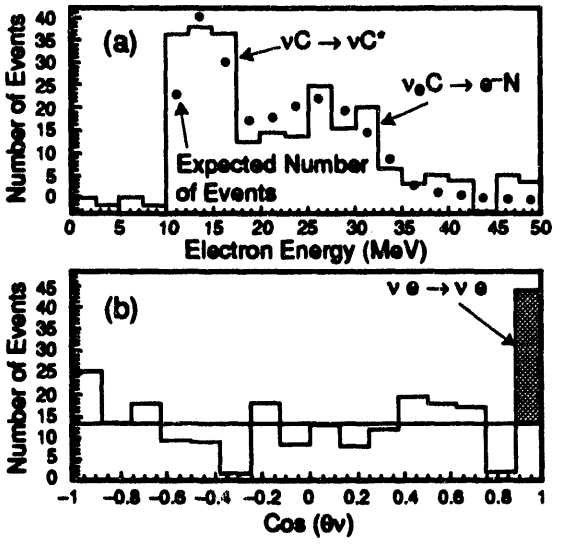

Figure 2. (a) The electron energy spectra from $\nu_e\ ^{12}C \rightarrow e^-\ ^{12}N$ scattering, $\nu_e\ ^{13}C \rightarrow e^-\ ^{13}N$ scattering, and $\nu e \rightarrow \nu e$ elastic scattering, where the neutrinos arise from π^+ and μ^+ decays at rest. (b) The $\cos\theta$ distribution, where θ is the angle between the electron direction and the incoming neutrino direction. The excess of events near $\cos\theta = 1$ is due to $\nu e \rightarrow \nu e$ elastic scattering.

A signature for a $\bar{\nu}_e$ interaction in the detector is the reaction $\bar{\nu}_e p \rightarrow e^+ n$ followed by $np \rightarrow d\gamma$ (2.2 MeV). This signature is, therefore, two-fold: a relatively high energy electron with more than 300 hit phototubes (>20 MeV) and a 2.2-MeV γ, which is in time-coincidence (within 0.5 ms) and position-coincidence (within 2.0 m) of the electron. The efficiency for the neutron to be captured by a free proton and for the 2.2-MeV γ to be reconstructed within 0.5 ms and 2.0 m and to have between 21 and 50 hit phototubes is 80%, and the probability of an accidental γ coincidence is 13% averaged over the detector. The γ reconstruction has been checked by selecting cosmic-ray neutrons with associated 2.2-MeV γs. Figure 3 displays for these cosmic neutron events the number of hit phototubes associated with the γ, the time difference between the γ and neutron, and the distance between the γ and neutron reconstructed positions. As can be seen in the figure, 2.2-MeV γs hit on average 33 phototubes, have a mean capture time of about 190 μs, and are reconstructed usually within 2 m of the parent neutron.

Figure 4 shows the electron energy distribution, the excess of beam on over beam off, for events that satisfy the electron selection criteria and with an associated 2.2-MeV γ. The histogram is the data and the dots show the expected background from $\nu_e C \rightarrow e^- N$ scattering and other known neutrino interactions. The electron selection criteria required that the event was consistent with a $\beta \sim 1$ particle, the reconstructed position (of the track midpoint) was >75 cm from the cylindrical surface of phototube faces, there were no veto shield hits in coincidence with the electron event, and there were no

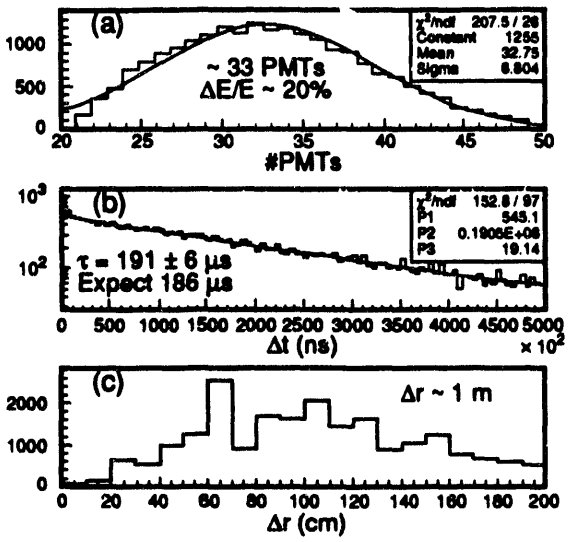

Figure 3. A sample of cosmic neutron events with associated 2.2-MeV γs. (a) The number of hit phototubes associated with the γ. (b) The time difference between the γ and neutron. (c) The distance between the γ and neutron reconstructed positions.

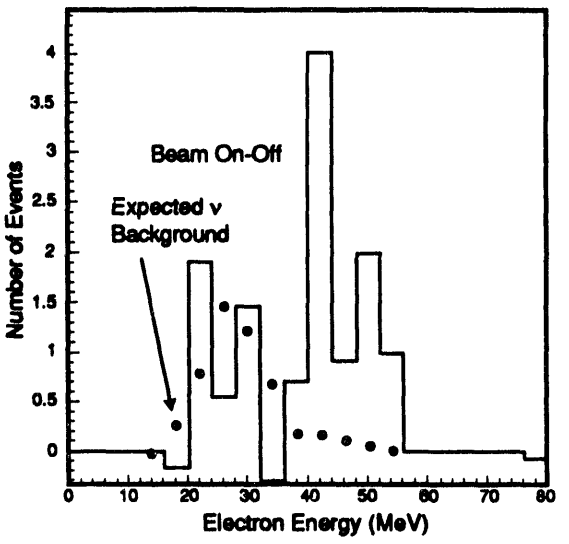

Figure 4. The electron energy distribution, beam on-off, for events that satisfy the electron selection criteria and that have an associated 2.2-MeV γ. The histogram is the data and the dots show the expected background from known neutrino interactions.

associated activity events 50 μs prior to the event. The electron selection efficiencies are given in Table 1; the overall electron selection efficiency is 26 ± 2%. Eight events are observed in the $38 < E_e < 56$ MeV energy range that are more than can be explained by conventional processes. This energy range is chosen because it is above the $\nu_e\ ^{12}C \rightarrow e^-\ ^{12}N$ background, as seen in Fig. 2(a). If the electron selection criteria are relaxed by decreasing the fiducial volume cut to 50 cm, by allowing up to two in-time veto shield hits, or by reducing the no-associated-activity cut to 40 μs, then the background increases slightly but the event excess remains.

Table 2 lists all of the backgrounds with the expected number of background events in the $38 < E_e < 56$ MeV energy range. The non-beam-related background is precisely determined from data collected with the beam off (the 7% duty factor results in 13 times more beam-off data than beam-on data). A severe limit is obtained for beam-induced neutrons by looking for a beam on-off excess for a sample of events consistent

Table 1
The electron selection efficiencies for electrons in the $38 < E_e < 56$ MeV energy range

Requirement	Efficiency
Event consistent with $\beta \sim 1$	0.80 ± 0.04
No veto shield hits	0.67 ± 0.02
No associated activity events	0.49 ± 0.04
Trigger deadtime	0.98 ± 0.01
TOTAL	0.26 ± 0.03

Table 2
A list of all backgrounds with the expected number of background events in the $38 < E_e < 56$ energy range. The neutrinos are from either π and μ decay at rest (DAR) or decay in flight (DIF).

Background	Neutrino Source	Number of Events
Beam Off		0.46 ± 0.19
Beam Neutrons		<0.020
$\bar{\nu}_e p \to e^+ n$	$\mu^- \to e^- \nu_\mu \bar{\nu}_e$ DAR	0.15 ± 0.04
$\nu_\mu C \to \mu^- X$	$\pi^+ \to \mu^+ \nu_\mu$ DIF	0.06 ± 0.03
$\bar{\nu}_\mu p \to \mu^+ n$	$\pi^- \to \mu^- \bar{\nu}_\mu$ DIF	0.04 ± 0.02
$\nu_e\ ^{13}C \to e^-\ ^{13}N$	$\mu^+ \to e^+ \bar{\nu}_\mu \nu_e$ DAR	0.06 ± 0.03
$\nu e \to \nu e$	$\mu^+ \to e^+ \bar{\nu}_\mu \nu_e$ DAR	0.056 ± 0.010
$\nu e \to \nu e$	$\pi \to \mu \nu_\mu$ DIF	0.008 ± 0.002
$\nu_e C \to e^- X$	$\pi \to e \nu_e$ DAR	0.009 ± 0.004
$\nu_\mu C \to \pi X$	$\pi \to \mu \nu_\mu$ DIF	0.012 ± 0.006
$\nu_e C \to e^- X$	$\pi \to e \nu$ DIF	0.004 ± 0.003
$\nu_e C \to e^- X$	$\mu \to e \nu \bar{\nu}$ DIF	0.005 ± 0.003
TOTAL		0.88 ± 0.20

with particles below Čerenkov threshold. The lack of such an excess allows us to place an upper limit on beam-induced neutrons relative to cosmic-ray-induced neutrons of <4% in the LAMPF beam spill. As the total beam off background is measured to be small, the beam on neutron background is negligible. The largest neutrino background is due to μ^- decay at rest in the A6 beam stop followed by $\bar{\nu}_e p \to e^+ n$ scattering in the detector. This background, which has a relatively large cross section [6], is suppressed by several factors that are calculated precisely by our beam simulation [4]: the π^-/π^+ ratio (0.14), the probability of π^- decay in flight (0.03), and the probability of μ^- decay at rest before capture (0.10). The total background due to μ^- decay at rest is, therefore, about 0.15 events. Another important background is due to the reactions $\nu_\mu C \to \mu^- X$ and $\bar{\nu}_\mu p \to \mu^+ n$, where either the muon is below the activity threshold (<18 hit phototubes) so that it is not read-out as an activity trigger or the Michel electron is missed and the muon is identified as an electron. This background can be accurately determined from our measurement of $\nu_\mu C \to \mu^- X$ [7]. From the total sample of 216 events, it is estimated that the number of events with either the muon or electron missed and a 2.2-MeV γ in coincidence is 0.10 events. This background estimate includes possible trigger inefficiency and cases where the muon decays promptly into an electron so that the event looks like a single particle. Other backgrounds arise from $\nu e \to \nu e$ scattering, $\nu_e\ ^{13}C \to e^-\ ^{13}N$ scattering, where the cross section estimate of Donnelly [8] is used, and $\nu_e\ ^{12}C \to e^- X$ scattering at higher energy, where the Fermi Gas Model cross section [5] is employed. The total estimated background is 0.9 ± 0.2 events, which results in a net excess of 7.1 ± 0.2 events in the $38 < E_e < 56$ MeV energy range.

4. CONCLUSION

The LSND experiment observes after an initial month-and-a-half run eight electron events in the 3 8 < E_e < 56 MeV energy range, which are in time and spatial coincidence with a low energy γ. The total estimated background from conventional processes is 0.9 ± 0.2 events, whereas 700 events are expected for maximal $\bar{\nu}_\mu \rightarrow \bar{\nu}_e$ oscillations. The LSND experiment will collect an order of magnitude more data over the next two years, which should allow an unambiguous interpretation of this excess.

REFERENCES

1. The LSND Collaboration consists of the following people and institutions: K. McIlhany, I. Stancu, W. Strossman, G. J. VanDalen (Univ. of California, Riverside); W. Vernon (Univ. of California, San Diego and IIRPA); D. Bauer, D. Caldwell, A. Lu, S. Yellin (Univ. of California, Santa Barbara); D. Smith (Embry-Riddle Aeronautical Univ.); A. Eisner, M. Sullivan, Y. Wang (Univ. of California IIRPA); I. Cohen (Linfield College); R. D. Bolton, R. Burman, J. Donahue, F. Federspiel, G. T. Garvey, W. C. Louis, V. Sandberg, M. Schillaci, D. H. White, D. Whitehouse (Los Alamos National Laboratory); R. Imlay, W. Metcalf, R. M. Gunasingha (Louisiana State Univ.); B. Boyd, K. Johnston (Louisiana Tech Univ.); B. B. Dieterle, R. Reeder (Univ. of New Mexico); M. Albert, J. Hill, A. K. Mann (University of Pennsylvania); A. Fazely (Southern Univ.); C. Athanassopoulos, L. B. Auerbach, V. Highland, J. Margulies, D. Works, Y. Xiao (Temple Univ.).
2. J. J. Napolitano et al., *Nucl. Instrum. Methods A* **274** (1989) 152.
3. R. A. Reeder et al., *Nucl. Instrum. Methods A* **334** (1993) 353.
4. R. L. Burman, M. E. Potter, and E. S. Smith, *Nucl. Instrum. Methods A* **291** (1990) 621.
5. T. K. Gaisser and J. S. O'Connell, *Phys. Rev. D* **34** (1986) 822.
6. P. Vogel, *Phys. Rev. D* **29** (1984) 1918.
7. M. Albert et al., submitted to *Physical Review Letters*.
8. T. W. Donnelly, *Phys. Lett.* **43B** (1973) 93.

DATE
FILMED
10/12/94

END